GLL
Geomatics, Landmanagement and Landscape No. 4 • 2025, 139–156

ISSN 2300-1496 https://doi.org/10.15576/GLL/214346

Research paper

Received: 4.11.2025
Accepted: 17.11.2025
Published: 30.12.2025

Assessment of the metrological properties of a handheld MLS point cloud for geodetic field surveys

Hubert Małyszek[1] 0009-0003-0823-344X
Przemysław Klapa[2,] ✉ 0000-0003-1964-7667
Bartosz Mitka[1] 0000-0002-1896-3126
Maria Zbylut-Górska[2] 0000-0003-4436-8248
Mateusz Zagórowski[3] 0009-0004-7460-0452

[1] Department of Rural Land Surveying, Cadastre and Photogrammetry, Faculty of Environmental Engineering and Geodesy, University of Agriculture in Krakow
[2] Department of Geodesy, Faculty of Environmental Engineering and Geodesy, University of Agriculture in Krakow
[3] Geodetic Students Society, Faculty of Environmental Engineering and Geodesy, University of Agriculture in Krakow,
✉ Corresponding author: przemyslaw.klapa@urk.edu.pl

Summary

A 3D point cloud is a collection of millions of spatial points that faithfully capture object shape and structure. Handheld mobile laser scanners are increasingly adopted because they enable rapid and complete acquisition. This paper evaluates the geometric and metrological quality of a point cloud collected with a handheld MandEye PRO scanner based on the Livox Mid-360 from an architectural object, using terrestrial laser scanning with a Leica ScanStation P40 and a network of total station control points as references. Point-like, linear, and planar features were assessed by registration to the control frame, segment-length comparisons, plane fitting, and cloud-to-cloud distance analysis. After registration, root mean square errors on control points fall within 0.02–0.19 m (mean 0.08 m). Segment lengths are consistent to within a single centimetre across handheld MLS, TLS, total station measurements, and direct field readings, while the differences in areas of fitted planes are 0.7–1.9%. Local deviations concentrate along edges and in shadowed zones, indicating sensitivity to trajectory coverage and sampling density. In well-covered regions, the overall agreement between MLS and TLS remains stable, whereas gaps in visibility or sparse sampling lead to localised discrepancies. The results show that, in this configuration, handheld mobile scanning provides accuracy consistent with the requirements

of geodetic documentation while offering high acquisition efficiency. These findings support the use of handheld MLS for architectural surveying and geodetic fieldwork, provided that route planning and sampling are designed to ensure robust coverage of critical facades, edges, and occluded areas.

Keywords

MLS • geodetic surveying • point cloud • geodetic instrument testing • accuracy assessment

1. Introduction

A point cloud is a discrete model of space composed of 3D points, usually in an XYZ system with attributes such as reflection intensity or RGB. In practice, the record is derived directly from the sensor's output format and accompanying IMU telemetry, which the manufacturer allows to be configured and acquired together with the cloud [Livox_Mid-360]. There are two types of point cloud sources: active and passive. Active sources include laser scanning, which provides direct distance measurements, while passive sources comprise image photogrammetry, where cameras (mono-, stereo-, multi-camera, RGB-D) are used to extract the position of points in space by matching images. These images also serve to colour point clouds. In mobile mapping systems, it is standard practice to combine LiDAR with cameras, and a GNSS/IMU set is used to determine the position of the platform or, in environments without GNSS, only IMU/vision odometry and control points [Elhashash et al. 2022]. The cloud resulting from laser scanning has a density and coverage that depends on the beam geometry, field of view and scanning pattern, as well as the reflectivity of the target and its location in the FOV. For Livox Mid-360, coverage within the FOV increases with integration time thanks to non-repeat scanning, which completes the scene and reveals details [Livox 2024].

Laser scanning in geoinformatics comprises three basic classes: ALS (airborne), TLS (terrestrial) and MLS (mobile). In ALS, the scanner is placed on a UAV or aircraft and performs acquisition from a nadir perspective, it effectively maps the upper parts of objects such as roofs or tree crowns, but has limited performance for vertical structures due to observation geometry and occlusion. TLS and MLS perform scanning from a horizontal perspective. In this paper, terrestrial systems are divided into stationary and mobile [Room and Ahmad 2023]. TLS is a ground-based static measurement with very high local resolution. The clouds it generates are dense and rich in detail, supporting geometric feature extraction and environmental analysis. MLS is a mobile system that combines LiDAR with navigation and efficiently maps vertical structures. Point clouds are used for roadside and urban area inventory tasks. It allows for the identification and measurement of elements such as curbs, signage, poles, power lines, vehicles, and the location and outline of buildings using planes and edges [Xia et al. 2020]. MLS is a measurement in motion with LiDAR-IMU data fusion and subsequent trajectory alignment, often with figure closure and georeferencing to GNSS or control points. It provides high performance in data acquisition and good completeness, but at the cost of greater sensitivity to drift and trajectory errors over long distances. In practice, the key features of MLS are: sensor integration (LiDAR+IMU, optional

cameras), odometry and SLAM algorithms with closure support, the ability to combine multiple sessions, and flexible georeferencing. Dynamic scanning is generally faster, usually slightly less accurate than static scanning, but enables effective documentation of objects with complex geometry and in difficult conditions [Noguchi et al. 2023]. The most important features of MLS with respect to quality are: speed of data acquisition with very high density, stable relative geometry, and accuracy dependent on GNSS/IMU conditions and control point strategy. In urban areas – with an obscured sky and sharp turns – local deformations can be directly indicated on deviation maps. These deformations are usually associated with poorer control point identification or temporary GNSS signal degradation [Běloch and Pavelka 2024].

Despite the development of modern technologies, classic measurement methods continue to be important for referencing results, verifying data quality, and conducting measurements in conditions of limited visibility or difficult measurement conditions. A hybrid approach is increasingly being used in practice. It combines traditional and modern measurement technologies, thereby increasing the precision and reliability of measurements [Krzan 2013]. Field measurement elements can be divided into three basic groups: point, line and surface objects. When measuring these elements, the focus lies on measuring points and their mutual position in space [Przegon 2016]. Polish national regulations specify that point objects are terrain elements with a precisely determined spatial location, including poles, hydrants and height benchmarks. These elements are mainly measured with electronic tachymeters or GNSS receivers operating in RTK or RTN modes, depending on the terrain conditions and the required accuracy of the survey. Linear objects include infrastructure elements such as water supply networks, gas pipelines, telecommunications cables, roads and fences. Their measurement requires the recording of break points in order to accurately map the course of the line in the terrain. Surface objects are mapped with contours from break points and densification points in order to accurately reflect the shape of plots, reservoirs, land cover or the surveyed surface. It must also be taken into account that a geodetic situational survey should guarantee a positional accuracy of no worse than 0.1 m for objects with the highest accuracy class (including construction objects and equipment, as well as elements of the site infrastructure); 0.3 m for objects and terrain details with less distinct contours or for underground objects and construction equipment, land development elements or earthworks and equipment, as well as terrain details whose unambiguous identification in the field is more difficult and depends on the assessment of the surveyor, e.g. land use contours, the course of watercourses, or the extent of water reservoirs – 0.5 m [Rozporządzenie 2020]. The basic solutions in classical geodesy for carrying out measurements in this regard are tachymetry and GNSS (in particular GNSS-RTK/RTN solutions). Tachymetry allows for the measurement of point objects with an accuracy of 0.02–0.05 m, depending on the accuracy of the measurement grid. However, it is independent of horizon obstruction, making it the preferred method in environments such as urban areas, forests or areas with limited satellite observation. On the other hand, GNSS measurements enable real-time coordinate acquisition with an accuracy of 0.03–0.05 m in favourable observation conditions. They offer an effective

solution for working in open and extensive areas, where the use of tachymetry would be too time-consuming [Karsznia 2008]. Tachymetry works better in cases where high observation precision is required, e.g. near terrain obstacles, utility network collisions or in the event of satellite signal interference [Siejka 2014]. TLS achieves measurement accuracy at the level of single millimetres; for example, for the Leica ScanStation P40, a point error of 3 mm/50 m horizontally and 6 mm/50 m vertically and a noise of 0.4–0.5 mm are specified. Meanwhile, the accuracy of MLS depends on the quality of the LiDAR-IMU trajectory and loop closures, georeferencing to control points, FOV coverage, and the distance and reflectivity of the target. In tests of the MandEye PRO scanner with a Livox Mid-360 sensor under laboratory conditions, MAE ≈ 0.013 m (static) and ≈ 0.017 m (dynamic) were obtained, as well as shape conformity of 10–15 mm, i.e. centimetre accuracy [Mitka et al. 2024].

The aim of the work is the geometric and metric validation of a point cloud obtained with a handheld MLS system over an architectural object in field surveying conditions. The verification was achieved by comparing the reference measurement with data from a terrestrial laser scanner with a higher accuracy class and tachymetric control, supplemented with selected measurements of lengths in the field. The following were evaluated: differences in MLS point coordinates relative to tachymetry after fitting, with determination of mean and RMSE errors; consistency of linear distances of representative elements of the object between MLS, TLS and tachymetry; the position of planes and the consistency of the position of objects on the object after fitting the planes; as well as the global consistency across MLS/TLS differential models, reported as the mean, standard deviation and point cloud distances. The objective articulated in this way allows for the assessment of the accuracy and usefulness of a handheld mobile laser scanner for surveying tasks, with particular emphasis on determining the location of objects, the reliability of dimensions, and the consistency of the shape of the documented surfaces.

2. Practical part

2.1. Field measurement – testing the measuring device

The MandEye PRO system (Fig. 1) is a mobile, handheld, low-cost MLS scanner based on the Livox Mid-360 head and integrated with IMU. The system was developed as an open, low-cost solution for rapid point cloud acquisition and subsequent processing in HDMapping software. A tool for inventorying sites and objects with centimetre accuracy and a high level of completeness and consistency of the point cloud [Mitka et al. 2024, Redovniković et al. 2024].

The Mid-360 head itself operates at a wavelength of 905 nm (class 1 laser) and scans in a non-repeating manner, which densifies the coverage in the field of view with every tenth of a second; in approx. 0.5 seconds, the FOV coverage reaches ~70%. The scanner's field of view is 360° horizontally and from −7° to 52° vertically (59° in total). The operating range of the device depends on reflectivity: ~40 m for 10% and up to ~70 m for 80%. The sensor has a distance measurement error of ≤ 0.02 m @ 10 m (up to 0.02 m @ 0.2 m)

and an angular error of ≤ 0.15°, with a typical stream of ~200,000 pts/s and 10 Hz. Inside, there is an IMU (3-axis accelerometer and gyroscope) with a 200 Hz output – useful for LiDAR-IMU odometry and trajectory estimation. The housing has an IP67 rating and an operating range of –20 to 55 °C [Livox 2024].

Source: Authors' own study

Fig. 1. MandEye PRO Mobile Laser Scanner (MLS): a. device; b. MLS in operation

Laboratory tests checked MLS – Mandeye against TLS Leica P40 (reference) and showed geometry accuracy in the order of single centimetres: cylinders ~10 mm in static mode and ~15 mm in motion mode, planes < 10 mm, corners ~10 mm in mobile mode; background noise 15–24 mm. Initial registration errors (MAE) were ~0.013 m for static mode and ~0.017 m for dynamic mode. This illustrates that the head itself operates correctly within centimetre accuracy [Mitka et al. 2024]. In field conditions for linear, elongated objects without closures (loop closures), it has been shown that differences can increase to decimetres due to very long trajectories, complex geometry and the method of georeferencing. Most points from the mobile scan differed from the static measurement by < 0.15 m (dominant classes 0.00–0.25 m, which, according to the authors, is acceptable for the purposes of mapping hard-to-reach objects, e.g. caves, and results, among other things, from the static shading of the measurement and different profile paths [Redovniković et al. 2024].

2.1.1. Research object

The building located on the URK campus at ul. Balicka 253C was chosen as the research object. It is a two-storey building with moderately complex geometry. Despite the

simple construction of the walls, it features many decorative elements that complicate digital reconstruction (Fig. 2).

Source: Authors' own study

Fig. 2. Surveyed object

2.1.2. Field research

The measurement works were conducted at the Faculty of Environmental Engineering and Geodesy of the University of Agriculture in Krakow and involved measuring a test object in the form of the URK manor house. The work was divided into two consecutive stages: acquisition of geospatial data using MLS, followed by measurement of control points, clearly identifiable on the surface of the test object, using a tachymeter. For reference and control survey purposes, measurements were also taken with a Leica ScanStation P40 terrestrial laser scanner (Fig. 3b).

Acquisition of geospatial data representing the building's external façade and visible roof sections was achieved using a MandEye PRO scanner. The measurement was conducted continuously, focusing on three complete circuits around the building, initially at a sensor height of approx. 1 metre above ground level and a distance of approx. 5 metres from the measurement object. Then the height was increased to approx. 1.5 m at a distance of approx. 15 m from the building, and finally at a height of approx. 2.5 m and a distance of approx. 25 m from the building. The scheme used was designed to ensure the widest possible coverage of the surveyed object, eliminating so-called dead zones - areas invisible from the given position of the scanner. The data was recorded in LAZ format, the default format for the used measuring device, and exported for further processing during office work.

The second stage of fieldwork focused on setting control points on the surface of the building. Due to the noise level of the employed scanner, instead of using control

points as target discs, mirrorless measurement of points in the form of objects clearly identifiable on the surface of the test object was assumed. For this purpose, a Leica TC307 tachymeter (Fig. 3a) with a prism for precision measurements was used. The measurements were taken from four previously established measurement grid points located around the building. Thirty-four points were measured, including building corners, facade elements, window lintels and decorative elements. The data in the form of XYZ coordinates in the local reference system was exported as a CSV file.

For reference and control measurements, a measurement was performed using a Leica ScanStation P40 terrestrial laser scanner (Fig. 3b).

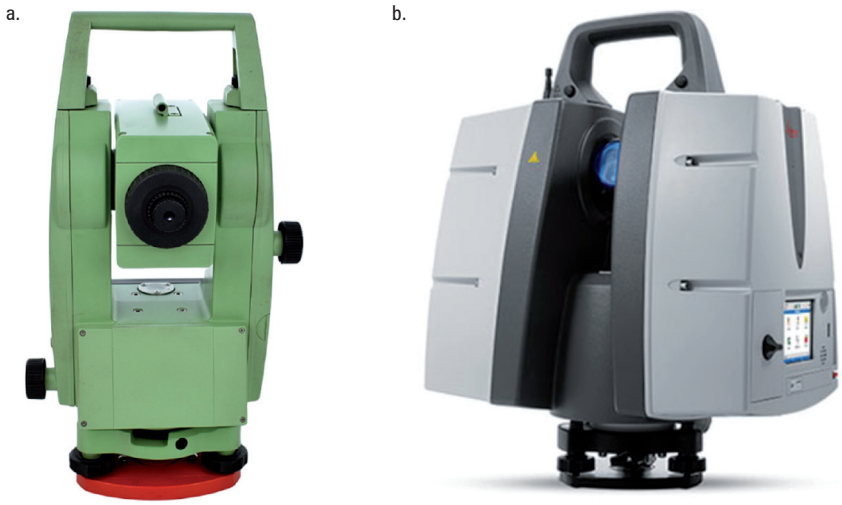

Source: Authors' own study

Fig. 3. Survey equipment used to verify MLS data: a. TC307 total station; b. TLS – Leica Scanstation P40

2.1.3. Processing of acquired survey data

The geospatial data obtained using the above-mentioned measuring devices were processed to identify common points, i.e. points that are uniquely identifiable for each of the used data sets. This was done in Cloud Compare software using the Point Picking tool, which allows coordinates in Euclidean space to be saved for selected points [Cloud Compare, ver. 2.6.1]. The reference base was taken from the points measured using the tachymetric method, on the basis of which spatial information on analogous points on the acquired point clouds was obtained. Next, using the Align tool (point pairs picking), corresponding points were assigned to each other, and then a transformation was performed to fit the clouds (Fig. 4). This operation generated reports containing data on the transformation matrix and scale factor, as well as the RMS error (Fig. 5).

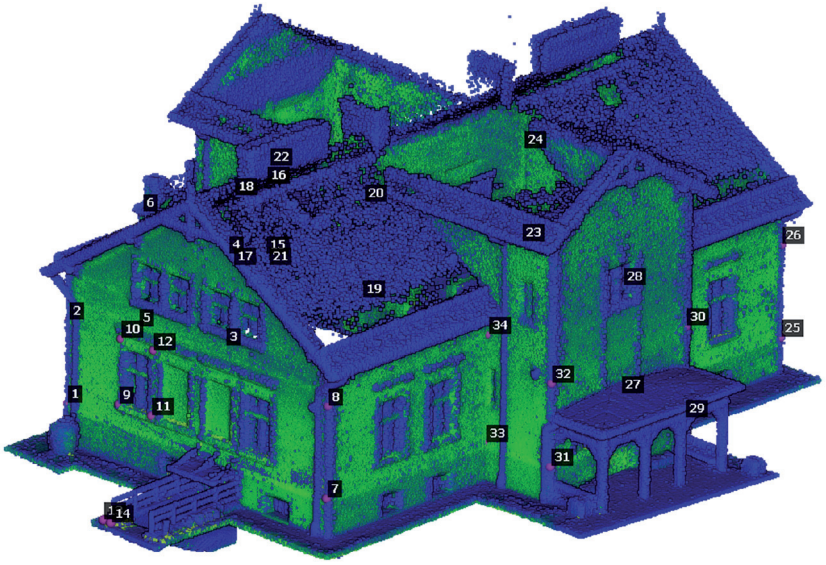

Source: Authors' own study

Fig. 4. MLS point cloud fitted to points surveyed using a total station (TLS – blue points, MLS – green points)

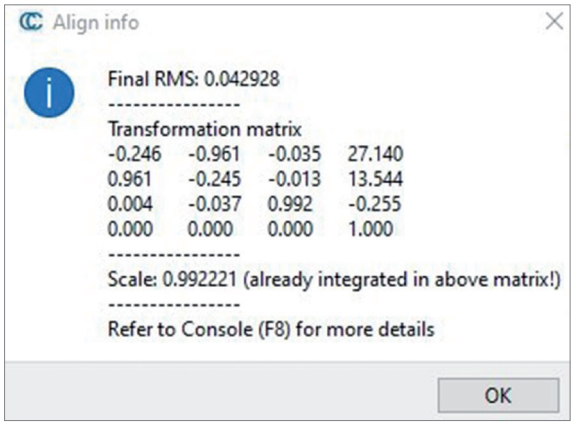

Source: Authors' own study

Fig. 5. The result of fitting the point cloud obtained using MLS to points measured using a tachymeter

Based on a point cloud fitted to a common reference system (compatible with tachymetry), measurement points were identified (Fig. 6).

A summary of the coordinate values of points from the MLS and the corresponding points surveyed using a total station is presented in Table 1.

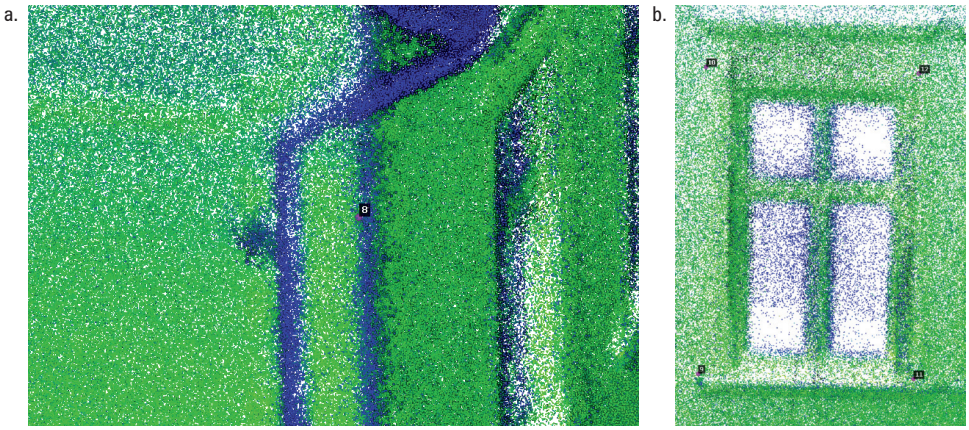

Source: Authors' own study

Fig. 6. Identification of points on the MLS cloud surface: a. for object corners; b. for characteristic points on object surfaces

Table 1. List and comparison of coordinate values for measurement points

	Total station			MLS			Accuracy of MLS position in relation to total station			Square error
ID	X	Y	Z	X	Y	Z	X	Y	Z	
1	18.271	12.572	1.030	18.254	12.608	0.960	−0.017	0.036	−0.069	0.08
2	18.271	12.577	4.232	18.291	12.624	4.176	0.020	0.047	−0.056	0.08
3	26.453	12.451	1.031	26.364	12.326	1.149	−0.089	−0.125	0.118	0.19
4	26.475	12.423	4.552	26.356	12.347	4.608	−0.119	−0.075	0.056	0.15
5	26.567	7.953	0.422	26.567	7.993	0.415	0.000	0.040	−0.007	0.04
6	26.627	7.979	4.832	26.543	7.937	4.846	−0.083	−0.041	0.014	0.09
7	18.463	25.490	1.041	18.447	25.507	1.040	−0.016	0.017	−0.001	0.02
8	18.474	25.471	4.586	18.442	25.468	4.564	−0.032	−0.004	−0.022	0.04
9	18.242	15.191	1.755	18.187	15.241	1.724	−0.056	0.050	−0.032	0.08
10	18.278	15.208	4.270	18.263	15.183	4.281	−0.016	−0.025	0.011	0.03
11	18.265	16.821	1.775	18.237	16.848	1.760	−0.028	0.027	−0.015	0.04
12	18.308	16.818	4.274	18.269	16.764	4.206	−0.039	−0.054	−0.068	0.10
13	13.630	19.060	−0.356	13.761	19.104	−0.403	0.132	0.044	−0.047	0.15
14	13.639	19.423	−0.356	13.757	19.462	−0.421	0.118	0.039	−0.065	0.14

Table 1. cont.

	Total station			MLS			Accuracy of MLS position in relation to total station			Square error
ID	X	Y	Z	X	Y	Z	X	Y	Z	
15	32.589	8.332	1.754	32.499	8.285	1.808	−0.090	−0.046	0.054	0.12
16	32.580	8.336	4.456	32.522	8.302	4.370	−0.058	−0.034	−0.086	0.11
17	30.919	8.336	1.772	30.956	8.324	1.778	0.037	−0.012	0.005	0.04
18	30.897	8.337	4.444	30.884	8.336	4.404	−0.012	−0.001	−0.039	0.04
19	33.460	12.350	1.010	33.556	12.335	1.021	0.096	−0.015	0.011	0.10
20	33.451	12.378	4.674	33.521	12.378	4.708	0.071	0.000	0.034	0.08
21	33.130	7.941	1.053	33.158	7.914	1.001	0.028	−0.026	−0.052	0.06
22	33.123	7.907	4.866	33.167	7.887	4.843	0.044	−0.019	−0.023	0.05
23	41.638	12.252	0.996	41.606	12.245	0.923	−0.033	−0.007	−0.074	0.08
24	41.629	12.268	4.553	41.601	12.321	4.447	−0.028	0.053	−0.106	0.12
25	41.809	25.166	0.986	41.837	25.163	1.030	0.027	−0.003	0.044	0.05
26	41.803	25.145	4.532	41.793	25.165	4.524	−0.009	0.020	−0.009	0.02
27	33.624	25.279	1.002	33.676	25.327	1.044	0.052	0.048	0.041	0.08
28	33.613	25.285	5.168	33.656	25.285	5.156	0.042	0.000	−0.011	0.04
29	33.662	28.480	0.980	33.730	28.496	0.985	0.068	0.016	0.005	0.07
30	33.633	28.455	4.499	33.688	28.450	4.545	0.055	−0.005	0.046	0.07
31	26.676	28.598	0.998	26.635	28.680	1.042	−0.041	0.082	0.043	0.10
32	26.687	28.572	4.182	26.619	28.588	4.158	−0.068	0.016	−0.023	0.07
33	26.630	25.398	1.004	26.569	25.420	1.057	−0.061	0.022	0.053	0.08
34	26.630	25.410	5.168	26.588	25.457	5.184	−0.042	0.047	0.016	0.07
									Mean:	0.08
									Standard deviation:	0.04

For length measurements, points marking the beginning and end of the measurement base on the object were identified (Fig. 7).

The obtained values of the lengths of the relevant sections are summarised in Table 2, and in Table 3, a list of differences for individual MLS-TLS-total station compilations is presented.

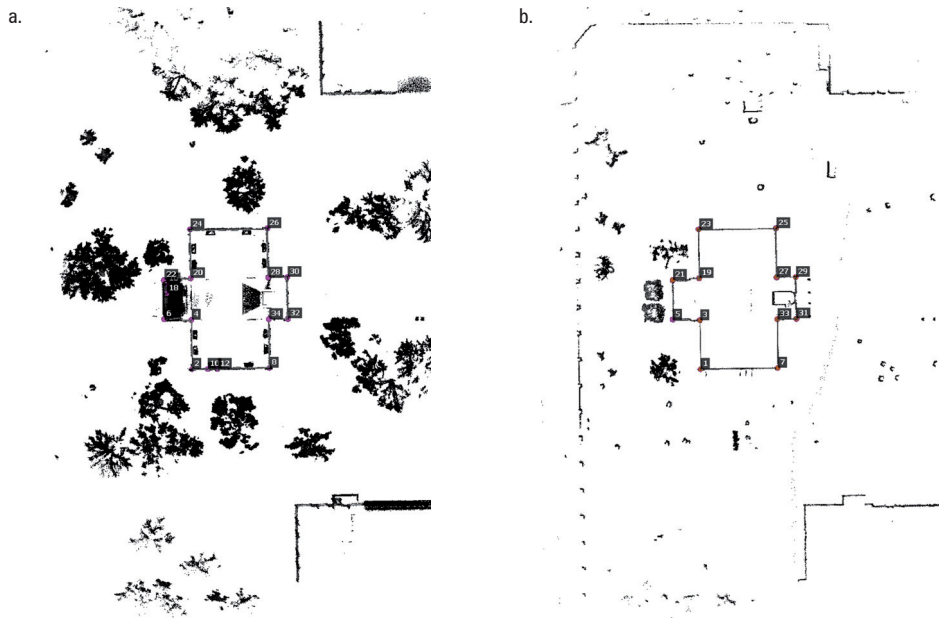

Source: Authors' own study

Fig. 7. Identification of measurement bases on horizontal cross-sections at the height of: a. the first floor; b. the ground floor

Table 2. Compilation of measured lengths

No.	Line	MLS [m]	TLS [m]	Total station [m]
1	29–31	6.94	7.06	7.07
2	31–33	3.17	3.17	3.17
3	33–7	8.19	8.14	8.13
4	7–1	12.88	12.86	12.85
5	1–3	8.18	8.09	8.08
6	3–5	4.48	4.53	4.50
7	5–21	6.49	6.63	6.63
8	21–19	4.44	4.42	4.41
9	19–23	8.20	8.10	8.08
10	23–25	12.89	12.86	12.85
11	25–27	8.16	8.16	8.15
12	27–29	3.16	3.14	3.13

Table 3. Compilation of differences in length values

No.	Line	Total station – MLS [m]	Total station – TLS [m]	MLS – TLS [m]
1	29–31	0.13	0.01	0.12
2	31–33	0.00	0.00	0.00
3	33–7	–0.06	–0.01	0.05
4	7–1	–0.03	–0.01	0.02
5	1–3	–0.10	–0.01	0.09
6	3–5	0.02	–0.03	–0.05
7	5–21	0.14	0.00	–0.14
8	21–19	–0.03	0.00	0.02
9	23–25	–0.04	–0.01	0.03
10	25–27	–0.01	–0.01	0.00
11	27–29	–0.03	–0.01	0.02
Mean:		0.00	–0.01	0.01
Standard deviation:		0.07	0.01	0.07

2.1.4. Assessment of the geometric accuracy of MLS point clouds

Due to the fact that common points were taken as elements for integration, objects in the form of planes – wall fragments – were checked. To enable this approach in the case of tachymetric data, the 'fit (plane)' tool available in Cloud Compare software was used. With its support, planes in the form of grids were fitted to the points (Fig. 8), which were then sampled onto a point cloud with the "sample points on a mesh" function [CloudComare, manual ver. 2.6.1].

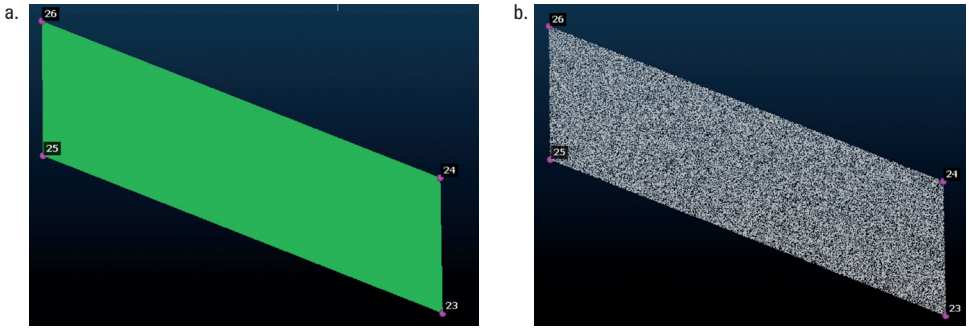

Source: Authors' own study

Fig. 8. Example of a plane created on the basis of: a. points from a total station; b. point cloud

In order to verify the geometric conformity between the planes created on the basis of tachymetric data and the data acquired using the MLS method, the 'cloud-to-cloud distance' tool was run in CloudCompare software. The source data was taken from previously created planes in the form of point clouds, obtained by sampling meshes. As a result of the algorithm, the distances between corresponding points of both sets were calculated, with results recorded as scalar values assigned to the tested cloud [CloudCompare Manual, ver. 2.6.1]. The obtained results were presented in the form of visualisations and histograms of deviation distribution, which allowed for the analysis of differences and assessment of the accuracy of the match (Fig. 9).

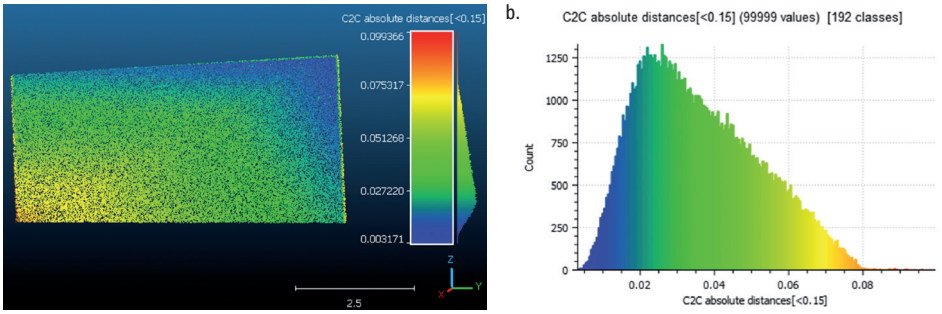

Source: Authors' own study

Fig. 9. Analysis of distances between planes created on the basis of points obtained with MLS and total station: a. differential model; b. histogram of distance distribution

A similar fit analysis was carried out for all walls – a geometric and metric assessment of the point cloud from MLS in relation to the values from the tachymetric survey (Fig. 10).

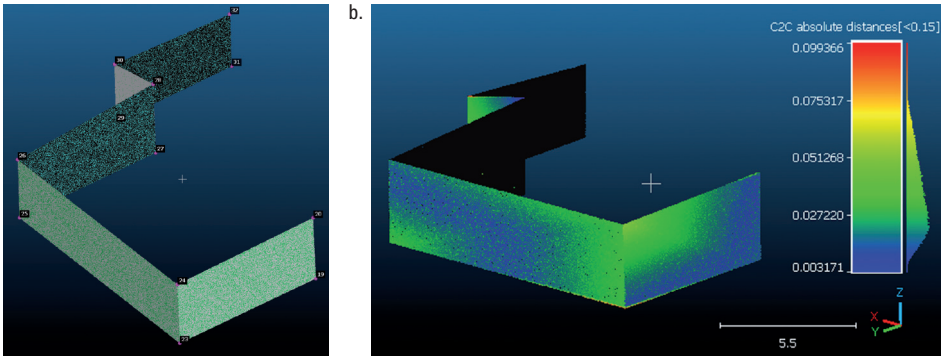

Source: Authors' own study

Fig. 10. Analysis of the distribution of distances between the planes created by MLS/total station: a. analysed planes; b. distribution of distance differences

The next stage involved analysing the surface area values for individual planes (walls) of the building. Statistical analysis of changes in surface area differences was conducted for the collected data (Table 4).

Table 4. Differences between MLS surface areas and total station measurements

Surface points	Tachymetry – surface area [m²]	MLS – area [m²]	Surface area differences [m²]	Difference in value [%]
32-31-30-29	23.322	22.907	−0.415	1.8
30-28-27-29	12.242	12.158	−0.084	0.7
28-27-25-26	29.491	29.115	−0.376	1.3
24-23-25-26	45.735	45.214	−0.521	1.1
20-19-23-24	31.573	30.987	−0.586	1.9
			Mean:	1.4

The next stage of the analysis was to assess the geometric properties of the point cloud from MLS. Data from terrestrial laser scanning (Leica P40) was taken as the reference base. Cloud-to-cloud fitting was performed (Fig. 11). A differential model was created for the point cloud from MLS and TLS (as a reference) (Fig. 12), presenting the relative distribution of values for individual points in the cloud.

The analysis of possible geometric changes in the point cloud was followed visually based on MLS/TLS point clouds and relevant common cross-sections through the cloud for the entire object (Fig. 13).

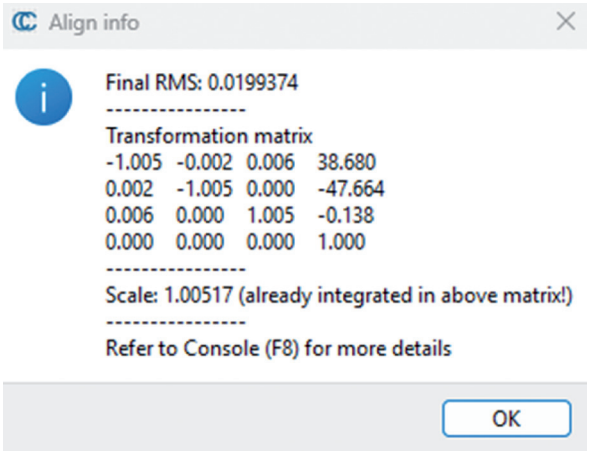

Source: Authors' own study

Fig. 11. Report on the matching of MLS point clouds with TLS

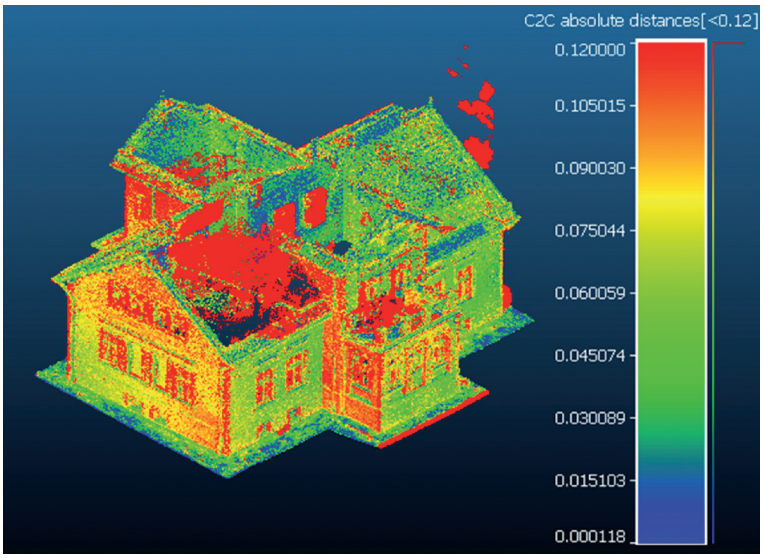

Source: Authors' own study

Fig. 12. MLS/TLS differential model

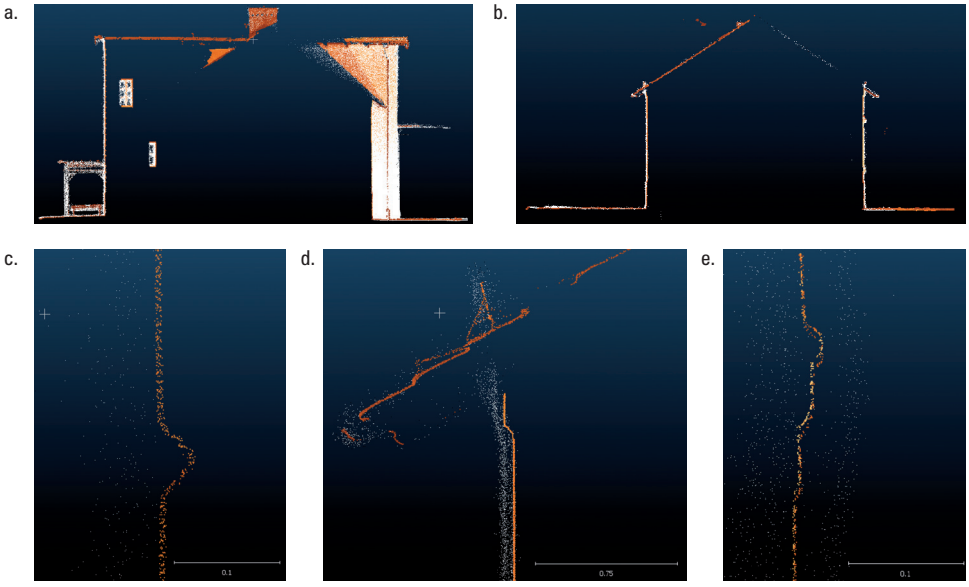

Source: Authors' own study

Fig. 13. Difference in changes in the position of objects – geometric assessment of points in the cloud from MLS (white) relative to TLS (orange), for: a. cross-section through the building; b. longitudinal section through the building; c. detail; d. roof structure; e. decoration

3. Result and discussion

The analysis covered the identification of features: point, line and plane measurements, as well as global verification of the point cloud from MLS. Control points and features were selected over sharp edges, corners and details with unambiguous definitions. In the MLS cloud, the position of a point was estimated as the average position of the local neighbourhood of points, while for curvilinear features it was determined by the intersection of fitted planes or lines. This selection limits the impact of noise and errors in individual samples. In point measurements, location uncertainty was assessed based on the deviation of point position values. The RMS values after fitting to the total station network are in the range of 0.02–0.19 m, with an average of approximately 0.086 m and a median of 0.08 m. The average components are approximately $\Delta X = -0.044$ m, $\Delta Y = -0.006$ m, $\Delta Z = 0.000$ m, which indicates a small directional component in the X-axis and no significant height shift. The highest RMS values are observed in areas with poor trajectory coverage and sharp changes in direction.

In linear measurements, lengths were determined directly between points and indirectly from the intersections of shapes and geometric structures. The indirect method is more resistant to noise and better reflects the architectural dimension for longer sections. The MLS is consistent with TLS and tachymetry to within centimetres for most sections. Cases of decimetre-level divergencies are mainly due to ambiguous identification of section ends or a local lack of cloud points.

In the plane analysis, the least squares method was used for fitting after filtering the deviations. The differences in area between the reference model and MLS are 0.084–0.586 m², which corresponds to 0.7–1.9%, averaging approximately 1.36%. The predominance of negative differences on the MLS side is due to the erosion of the envelope at the edges caused by lower sampling density, deviation filtering and extreme angles of incidence. Cloud-to-cloud distance maps show distributions concentrated around zero in bands with stable coverage and longer tails in niches, under cornices and on sharp corners. In global terms, the compatibility of MLS with TLS is good in areas of stable coverage and deteriorates locally with sharp turns in the trajectory and shading. In practice, it is recommended to design the route with loops and returns along key elevations, increase the sampling density in edge areas and prefer point identification by barycentre or primitive intersections. Measurements conducted in this manner provide reliable point, line and plane results on a scale of 'several centimetres', and enable effective integration with TLS and tachymetry data.

Therefore, a multi-sensor measurement approach is becoming a good standard, combining classical surveying methods, such as tachymetry and levelling, with GNSS satellite measurements and complementary techniques (TLS or photogrammetry). This makes it possible to capture both the basic geometry of the object and its full detailed features, while maintaining data consistency. Tachymetry provides point accuracy of ±0.02 m and serves not only as a tool for measuring points, but also as a reference base for verifying coordinates and segment lengths. Terrestrial

laser scanning, on the other hand, provides a 3D cloud with known resolution and high completeness and consistency of the acquired data, useful for shape conformity assessment and surface control. Research on the integration of geodetic measurements [Klapa et al. 2025, Gawronek et al. 2024] has shown that comparing coordinates from TLS and tachymetry with other data sources results in high consistency of information. Tachymetry provides reliable point reference and length control, while TLS provides surface reference and preserves the geometry of objects. Together, they enable reliable assessment of the metric and geometric consistency of data from other sources, including MLS [Klapa et al. 2025, Gawronek et al. 2024]. The results are consistent with observations from the literature on the subject: handheld MLS achieves accuracy to the centimetre in controlled conditions, while local deviations may occur in complex scenes and over long distances. Key factors include route design (loops, closures), control point placement, and coordination with reference measurements. TLS matches the density and stability of geometry for detail, while MLS provides significantly higher performance and completeness in a short time.

4. Conclusions

The handheld MLS (MandEye/Livox Mid-360) confirmed its usefulness for inventorying/documenting architectural objects in situational measurement standards: after fitting into the total station network, centimetre-level accuracy was achieved in point, line and plane measurements, as well as correct global consistency in areas with good trajectory coverage. Control statistics are in the range of 0.02–0.19 m (RMS), with an average of ≈0.08 m and a median of 0.08 m; a small directional component is noticeable in the X-axis ($\Delta X \approx -0.04$ m, $\Delta Y \approx -0.01$ m, $\Delta Z \approx 0.00$ m), without significant height displacement.

In linear relationships, where lengths were determined directly from pairs of points and indirectly from intersections of geometric primitives, consistency between MLS and TLS and tachymetry was achieved at centimetre level. Observations of the decimetre order were incidental and resulted from ambiguous identification of segment ends or insufficient local point cloud coverage. In the plane analysis, the area differences between the reference model and MLS are 0.7–1.9% (average ≈1.4%). The predominance of negative values on the MLS side indicates erosion of the envelope at the edges associated with sampling density and deviation filtering. C2C distance maps show distributions clustered around zero in areas with stable coverage and elongated tails in niches, under cornices and at sharp corners.

The accuracy of MLS is determined by FOV coverage and course of the route, therefore loops and 'returns' along key elevations, higher sampling density in edge zones, and defining features as barycentres of neighbourhoods or intersections of stable primitives are recommended. In terms of methodology, the most advantageous approach remains a multi-sensor approach, combining MLS as a fast source of a complete cloud with TLS for detail and tachymetry as an independent point control.

References

Běloch L., Pavelka K. 2024. Optimizing Mobile Laser Scanning Accuracy for Urban Applications: A Comparison by Strategy of Different Measured Ground Points. Appl. Sci., 14, 3387. https://doi.org/10.3390/app14083387

CloudCompare, Manula, version 2.6.1. https://www.cloudcompare.org/doc/qCC/CloudCompare%20v2.6.1%20-%20User%20manual.pdf [accessed: 30.10.2025].

Elhashash M., Albanwan H., Qin R. 2022. A Review of Mobile Mapping Systems: From Sensors to Applications. Sensors, 22, 4262. https://doi.org/10.3390/s22114262

Gawronek P., Klapa P., Sochacki D., Piaseczna K. 2024. Multi-Platform Collaboration in Integrated Surveying: Ensuring Completeness and Reliability of Geospatial Data – A Case Study. Remote Sens., 16, 4499. https://doi.org/10.3390/rs16234499

Karsznia K. 2008. Koncepcja pomiaru i wyrównania przestrzennych ciągów tachimetrycznych w zastosowaniach geodezji zintegrowanej. Acta Sci. Pol., Geod. Descr. Terr., 7(1), 35–46.

Klapa P., Gawronek P., Gargula T., Sokołowska A., Sajdak K. 2025. Integrating surveying, photogrammetric, and remote sensing data to generate large-scale maps. Archives of Civil Engineering, 71, 37–50. https://doi.org/10.24425/ace.2025.154106

Krzan G. 2013. Technologia zintegrowanych pomiarów klasycznych i satelitarnych GPS. Biuletyn Wojskowej Akademii Technicznej, 62(4), 47–61.

Livox. 2024. Livox Mid-360, User Manual v1.2.

Mitka B., Klapa P., Gawronek P. 2024. Laboratory tests of metrological characteristics of a non-repetitive low-cost mobile handheld laser scanner. Sensors, 24, 6010. https://doi.org/10.3390/s24186010

Noguchi A., Nakamura R., Takata Y., Matsuo Y., Oya Y., Uchida S. 2023. Comparison and evaluation of TLSs and mobile LiDAR scanners for multi-scale 3D documentation of cultural heritage. Int. Arch. Photogramm. Remote Sens., Spatial Inf. Sci. XLVIII-M-2-2023, 1135–1139. https://doi.org/10.5194/isprs-archives-XLVIII-M-2-2023-1135-2023

Przegon W. 2016. Geodezja rolna i architektura krajobrazu w kształtowaniu przestrzeni rurystycznej. Teoria, badania, aplikacje. Wydawnictwo Uniwersytetu Rolniczego w Krakowie, Kraków.

Redovniković L., Jakopec A., Będkowski J., Jagetić J. 2024. The affordable DIY Mandeye LiDAR system for surveying caves, and how to convert 3D clouds into traditional cave ground plans and extended profiles. International Journal of Speleology, 53(3), ijs2535. https://doi.org/10.5038/1827-806X.53.3.2535

Room M.H.M., Ahmad A. 2023. Fusion of UAV-based LiDAR and mobile laser scanning data for construction of 3D building model. Int. Arch. Photogramm., Remote Sens. Spatial Inf. Sci. XLVIII-4/W6-2022, 297–302. https://doi.org/10.5194/isprs-archives-XLVIII-4-W6-2022-297-2023

Rozporządzenie Ministra Rozwoju z dnia 18 sierpnia 2020 r. w sprawie standardów technicznych wykonywania geodezyjnych pomiarów sytuacyjnych i wysokościowych oraz opracowywania i przekazywania wyników tych pomiarów do państwowego zasobu geodezyjnego i kartograficznego. Dz.U. 2020, poz. 1429.

Siejka Z. 2014. Szybkie pozyskiwanie precyzyjnych i wiarygodnych informacji geodezyjnych w czasie rzeczywistym na potrzeby inżynierii środowiska. Acta Scientiarum Polonorum, Formatio Circumiectus, 13(3), 79–90. https://doi.org/10.15576/ASP.FC/2014.13.3.79

Xia S., Chen D., Wang R., Li J., Zhang X. 2020. Geometric Primitives in LiDAR Point Clouds: A Review. IEEE Journal of Selected Topics in Applied Earth Observations and Remote Sensing, early access. https://doi.org/10.1109/JSTARS.2020.2969119